

Availability of Free-Space Laser Communication Link with the Presence of Clouds in Tropical Regions

Thang V. Nguyen¹, Hoa T. Le¹, Hien T. T. Pham¹, and Ngoc T. Dang^{*,1}

¹Wireless Systems and Applications Lab., Posts and Telecommunications Institute of Technology, Hanoi 100000, Vietnam

Abstract

Free-space laser communication (lasercom), a great application of using free-space optics (FSO) for satellite communication, has been gaining significant attraction. However, in spite of great potential of lasercom, its performance is limited by the adverse effects of atmospheric turbulence and cloud attenuation, which directly affect the quality and availability of lasercom links. The paper, therefore, concentrates on evaluating the cloud attenuation in the FSO downlinks between satellite and ground stations in tropical regions. The meteorological ERA-Interim database provided by the European Center for Medium-Range Weather Forecast (ECMWF) from 2015 to 2020 is used to get the cloud database in several areas in tropical regions. This study proposed a novel probability density function of cloud attenuation, which is validated by using a well-known curve-fitting method. Moreover, we derive a closed-form of satellite-based FSO link availability by applying the site diversity technique to improve the system performance. Numerical results, which demonstrate the urgency of the paper, reveal that the impact of clouds on tropical regions is more severe than in temperate regions.

Received on 10 May 2023; accepted on 19 August 2023; published on 23 August 2023

Keywords: Satellite communications, Free-space laser communications (lasercom), Cloud attenuation, Atmospheric turbulence, Site diversity technique

Copyright © 2023 T. V. Nguyen *et al.*, licensed to EAI. This is an open access article distributed under the terms of the Creative Commons Attribution license (<https://creativecommons.org/licenses/by/4.0/>), which permits unlimited use, distribution and reproduction in any medium so long as the original work is properly cited.

doi:10.4108/eetinis.v10i3.3327

1. Introduction

Technology, more than ever, has been tightly getting involved in our daily basis and work. Human has been craving more information and connections anytime and anywhere to support their lives at most. All the seemingly essential needs have pushed the massive development in telecommunication. Shortly, 6G has been considered a promising network to satisfy the ubiquitousness of the Internet connection. In 6G, the huge development is not limited to terrestrial networks, but also satellite networks. They supplement existing terrestrial networks due to their cost-effective, rapid deployment, which is easily achieved from the popularity of low-earth orbit (LEO) satellites [1–3]. On the other hand, free-space laser communication (lasercom) using large optical bandwidth can transmit extremely

high data rates and better security over long transmission distances without exhausting precious and limited radio frequency (RF) resources [4]. Therefore, the effective combination of satellite communication and FSO technology, also well known as lasercom, is expected to be one of the key technologies in 6G [5].

Lasercom, with its rapid deployment ability, helps to ensure the ubiquitousness of 6G not only in general and smooth conditions but also in some unexpected and challenging conditions caused by natural disasters such as hurricanes, floods, and earthquakes. In the world, Asia, unfortunately, suffers the majority of disasters, more specifically, 40% of the whole [6]. Countries located in tropical regions, such as the Philippines, Indonesia, Vietnam, and so on, have higher disaster events as they are exposed to the sea with a long coastline. Their common feature is placed in a typical tropical region and is annually struck by either flood in mountainous areas or storms in coastal areas. Therefore, establishing and operating

*Corresponding author. Email: ngocdt@ptit.edu.vn

the infrastructure to continuously get data from satellites to monitor natural disasters and promptly take accurate response measures to reduce losses of life and property is a critical step and urgent. And it certainly can be achieved through utilizing free-space lasercom. However, lasercom remains some drawbacks because optical communication between satellites and earth stations is heavily influenced by weather conditions such as clouds and atmospheric turbulence [7, 8]. For this reason, it is extremely necessary to investigate the availability of optical communication links from satellites in specific locations to set up the design and implementation of satellite-based optical communication systems.

In recent years, a number of studies have focused on estimating the availability of optical communication systems in the presence of clouds because clouds cause a significant loss of optical signals in vertical links [7–11]. To do so, two methods have been proposed, including (1) using measurement devices at the ground station and (2) utilizing available databases. In the first method, Suzuki et al. observed link availability based on the image data of clouds collected by a whole-sky camera on the ground [9, 12, 13]. In these studies, the optical ground stations are implemented at ten locations at National Institute of Information and Communications Technology (NICT) facilities throughout Japan. The observed data is sent to the central station through a terrestrial network. The disadvantage of this method is that it requires high cost and complex systems, which are not always possible for all cases in different regions. The second approach is based on cloud liquid water content (CLWC) data from available databases observed by satellites [10]. The main advantage of this method is its ability to be implemented anywhere on Earth where we intend to place the optical ground station. Most of the previous works based on the CLWC concentrated on modeling the ON/OFF channel depending on the cloud coverage statistics without considering the cloud attenuation distribution [10, 11, 14, 15]. Based on the analysis algorithm in these studies, optical satellite links were evaluated to be interrupted whenever there is a presence of cloud coverage determined by CLWC data (with $CLWC > 0$). Nevertheless, as reported in [7, 10], the FSO-based satellite links can still be maintained in the presence of cloud coverage. The reason is that the attenuation due to clouds can be small enough when CLWC is not high. As a result, investigating and providing the cloud attenuation statistical model and link availability for FSO-based satellite communications are crucial and necessary. In [7, 8], the author analyzed the availability of optical communication links between satellites and several areas in temperate regions, e.g., Tokyo, Hokkaido, etc., based on the available data from the European

Center for Medium-Range Weather (ECMWF). And, the log-normal distribution is used to model the cloud database. The limitation of these studies is that it is only suitable for temperate regions and not universal for other climates, such as the tropical regions where cloud distribution is more complex.

In this study, we aim to explore the influence of clouds on FSO communication satellite systems in tropical regions. To do so, we first get the relevant database of weather conditions of tropical regions. We then derive a novel cloud attenuation statistical model, i.e., **the Gamma model**, based on the observed CLWC data from the ECMWF database of tropical regions. Next, the data will be used to estimate the availability of free-space lasercom links between satellites and ground stations located in tropical regions. Last but not least, we derive a closed-form to calculate the satellite-based FSO link availability by using the site diversity technique, which helps to improve the system performance.

The remainder of this paper is organized as follows. In Section 2, we present the free-space lasercom limitations, including atmospheric turbulence and cloud coverage. The matching cloud attenuation statistical model is derived in Section 3. Then, the system performance, i.e., link availability, is analyzed in Section 4. Section 5 discusses interesting numerical results. Finally, the key point of our work sum up, and the outlook for future work is provided in the conclusion section.

2. Free-Space Lasercom Limitations

This section will focus on two main challenges while implementing optical communication systems between satellites and ground stations. In particular, two random atmospheric conditions, including clouds and atmospheric turbulence, are investigated in our study.

2.1. Atmospheric Turbulence

Atmospheric turbulence is a random phenomenon caused by the inhomogeneity of atmospheric temperature and pressure along the transmission path. As a result, the received optical power strongly fluctuated due to the scintillation. Typically, the turbulent strength is determined by the Rytov variance, denoted by σ_R^2 , where the weak, moderate, and strong regimes corresponding to the Rytov variances as followed $\sigma_R^2 < 1$, $\sigma_R^2 \approx 1$, and $\sigma_R^2 > 1$ [16, 17]. In the vertical FSO communication, the Rytov variance in the case of plane wave propagation is determined as follows

$$\sigma_R^2 = 2, 25k^{\frac{7}{6}} \sec^{\frac{11}{6}}(\xi) \int_{H_g}^{H_{sat}} C_n^2(h) (h - H_g)^{\frac{5}{6}} dh \quad (1)$$

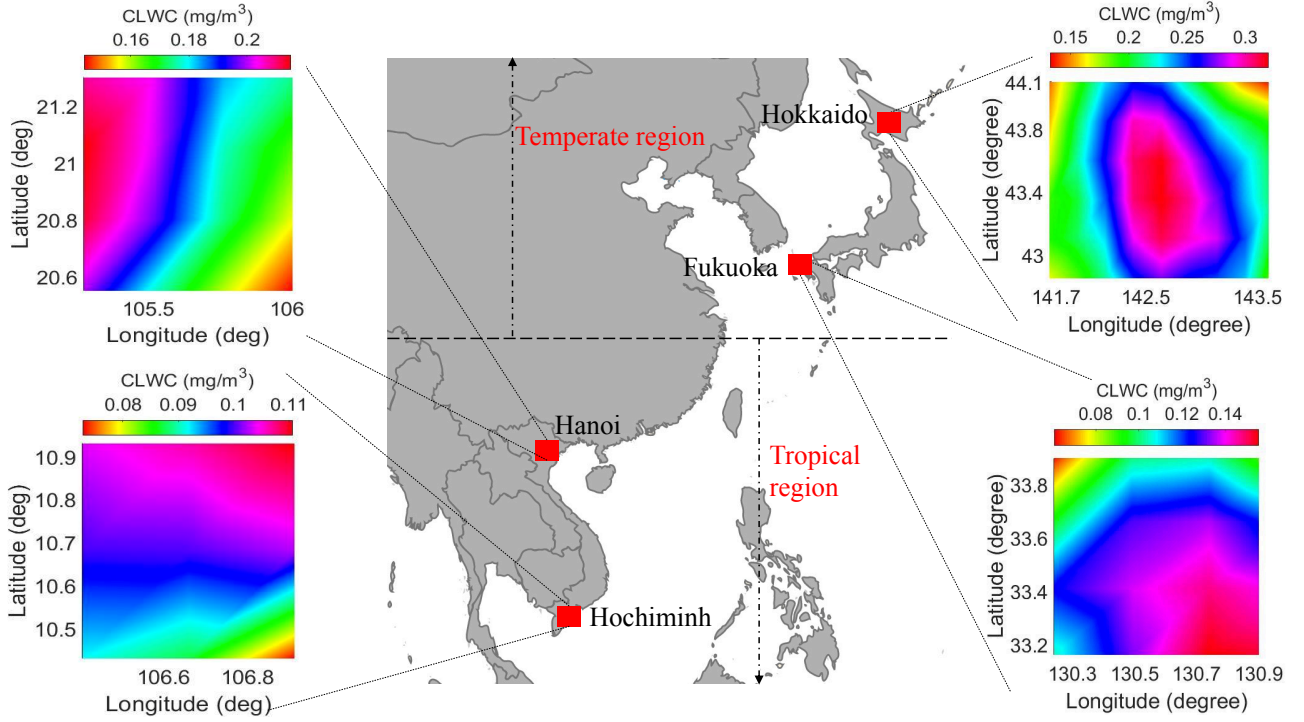


Figure 1. Difference of the cloud liquid water content (CLWC) in several areas in tropical regions (Hanoi and Hochiminh) and temperate regions (Hokkaido and Fukuoka) in the period 2015 – 2020.

where $k = 2\pi/\lambda$ is the number of optical waves, $\sec(\cdot)$ is the secant function, ξ is the zenith angle, H_g is the altitude of the ground stations, and H_{sat} is the satellite's altitude from the earth's surface. Compared with the horizontal FSO communication, the calculation of atmospheric turbulence becomes more complicated in the vertical case because the refractive index varies to the height [17]. The method of determining this index is presented by the formula below

$$C_n^2(h) = 0.00594 \left(\frac{v_{wind}}{27} \right)^2 (10^{-5}h) \exp\left(-\frac{h}{1000}\right) + 2.7 \times 10^{-16} \exp\left(-\frac{h}{1500}\right) + C_n^2(0) \exp\left(-\frac{h}{100}\right) \quad (2)$$

where $C_n^2(0)$ is the level of atmospheric turbulence at the ground level and usually varies between $10^{-17} m^{-2/3}$ (weak turbulence) and $10^{-13} m^{-2/3}$ (strong turbulence), and v_{wind} (m/s) is the root mean square value of wind speed with a typical value about 21 m/s [17, 18].

2.2. Cloud Attenuation

Clouds form when water vapor rises and condenses in the air as water droplets. These water droplets are tiny and light enough to float in the air. However, water droplets can freeze into ice crystals if they appear at a cold temperature due to different cloud heights from

the ground. Therefore, there are three main types: high-level, middle-level, and low-level clouds. Those types consist of only ice crystals, mainly ice crystals, and mainly water droplets, respectively. Among them, low-level clouds (under 3 km) affect optical signals the most because of Mie scattering, i.e., the size of a water droplet is much larger than the optical wavelength [7]. They become the main challenging issues for free-space lasercom links.

To investigate the impact of clouds on the free-space lasercom links, we analyze CLWC data from the available databases provided by the ERA-interim [19]. For the characterization of cloud attenuation statistics, the CLWC data is collected with the temporal solution of one sample per hour and a spatial resolution of $0.25^\circ \times 0.25^\circ$ latitude/longitude grid. Due to [7, 10] and the above explanation, only low-level clouds are investigated. The CLWC data is extracted from the cloud base altitude ($h_0 = 1$ km) to the cloud top altitude ($h_{top} = 3$ km) above the Earth's surface. The data for three different locations in Vietnam, including Hanoi (21.0142°N , 105.5115°E), Danang (16.0410°N , 108.1235°E), and Hochiminh (10.4632°N , 106.4207°E), are investigated. Figure 1 illustrates the average CLWC over some areas in tropical regions (Hanoi and Hochiminh) and several areas in temperate

regions (Hokkaido and Fukuoka) in the period 2015 – 2020.

Clouds affect both optical signal power and visibility by reducing their values significantly. As reported in [20, 21], the visibility, denoted as V , can be estimated as

$$V = \frac{1,002}{(W_c \times N_c)^{0.6473}}, \quad (3)$$

where W_c (g/m^3) is the cloud liquid water content. N_c (cm^{-1}) is the concentration of water content in the cloud; this parameter depends on the radius of the droplet in the cloud and can be determined as follows

$$N_c = \frac{3W_c}{4\pi r^3 \rho} \times 10^6, \quad (4)$$

where ρ ($= 1g/m^3$) is the density of the water content and r (μm) is the average radius of the droplet in the cloud. Depending on the type of cloud, the radius value can change; several typical values for some types of clouds are as follows: Stratus $r = 3.33\mu m$, Cumulus $r = 6.0\mu m$, and Nimbostratus $r = 4.7\mu m$ [22].

Given the visibility V (km) in (3) and by using the Kim model [23] to describe the cloud attenuation over the considered cloud layers, denoted as A_c (dB), then can be expressed as [7]

$$A_c = \sum_{k=1}^M 4.34 \left(\frac{3.91}{V_k} \left(\frac{\lambda}{550} \right)^{-\delta_k} \right) \frac{\Delta h_k}{\sin(\theta)}, \quad (5)$$

where λ is the laser's wavelength, θ is the satellite elevation angle, M is the total cloud layers considered, and Δh_k is the vertical extent of the k -th liquid cloud layer [20]. Here, $\sum_{k=1}^M \Delta h_k / \sin(\theta) = (h_{top} - h_0) / \sin(\theta)$ is the optical propagation path along which the Mie scattering phenomena happen. In addition, the coefficient δ , which is computed based on the size distribution of the scattering particles, is determined from empirical models [23] and specified by the Kim model as follows

$$\delta = \begin{cases} 1.6, & \text{if } V > 50, \\ 1.3, & \text{if } 6 < V \leq 50, \\ 0.16V + 0.34 & \text{if } 1 < V \leq 6, \\ V - 0.5 & \text{if } 0.5 < V \leq 1, \\ 0 & \text{if } V \leq 0.5, \end{cases} \quad (6)$$

where V (km) is the visibility [24]. Equation (6) implies that there will be less attenuation for any meteorological condition for higher wavelengths.

3. Cloud Attenuation Statistical Model

This section aims at modeling the distribution of cloud attenuation derived from the observed data of CLWC.

Several well-known analytically statistical models, such as gamma, gamma-gamma, chi-square, and exponential distribution models, are considered. Basically, two methods exist to find the best model, including interpolation and least-square fitting. Interpolation usually requires estimating intermediate values between precise data points; hence it is time-consuming, and it's hard to do for millions of data points. Therefore, we use the least-square fitting method to find the best-fitting curve by minimizing the sum of the square of the offsets of the points data.

To evaluate those models' accuracy, we apply a factor of determination denoted as R-square or R^2 statistic to assess the matching between considered distribution models and the collected data. Let $y = \{y_1, y_2, \dots, y_N\}$ and $f = \{f_1, f_2, \dots, f_N\}$ indicate as the measured data and estimated values, respectively, with N being the number of bins of the data histogram. Mathematically, the R-square coefficient can be given as

$$R^2 = 1 - \frac{SS_{res}}{SS_{tot}} = 1 - \frac{\sum_{i=1}^N (y_i - f_i)^2}{\sum_{i=1}^N (y_i - \bar{y})^2}, \quad (7)$$

where $SS_{res} = \sum_{i=1}^N (y_i - f_i)^2$ is the residual sum of squares, and $SS_{tot} = \sum_{i=1}^N (y_i - \bar{y})^2$ is the total sum of squares with $\bar{y} = \frac{1}{N} \sum_{i=1}^N y_i$ is the mean of observed data. It is important to note that the closer to 1 R^2 value is, the better matching between the estimated distribution and the observed data.

As seen in Table 1, the gamma distribution is the most suitable to model the cloud attenuation for all of the considered data sets extracted from the ECMWF database. As a result, the probability density function (PDF) of the cloud attenuation can be expressed as

$$f_{A_c}(A_c; \alpha, \beta) = \frac{(A_c/\beta)^{\alpha-1} \exp(-A_c/\beta)}{\beta \Gamma(\alpha)}, \quad A_c, \alpha, \beta > 0, \quad (8)$$

where $\Gamma(\cdot)$ is the Gamma function. Parameter α determines the shape of the gamma distribution function, while parameter β determines the scale of the function. Both parameters can be determined by using the maximum likelihood estimation curve-fitting method based on the data sets extracted from the ECMWF database.

4. Performance Analysis

This section will focus on analyzing the performance of a lasercom link by evaluating the system availability under the impact of two atmospheric problems (atmospheric turbulence and cloud attenuation) and different weather conditions. The value of system availability is achieved by comparing the total power loss caused by the above impact with a designed power budget. And then, the site diversity technique is proposed to improve the current system availability.

Table 1. Curve Fitting Evaluation, R^2 .

Season	Location	Gamma	Gamma-Gamma	Chi-square	Exponential
Spring	Hanoi	0.9684	0.7756	0.6905	0.6524
	Danang	0.9641	0.8070	0.6749	0.6274
	Hochiminh	0.9690	0.8485	0.7879	0.6816
Summer	Hanoi	0.9714	0.8247	0.7555	0.6831
	Danang	0.9788	0.7903	0.7097	0.7258
	Hochiminh	0.9675	0.6862	0.5757	0.6323
Autumn	Hanoi	0.9703	0.7340	0.4256	0.6709
	Danang	0.9757	0.6767	0.5620	0.6988
	Hochiminh	0.9749	0.6721	0.5569	0.6847
Winter	Hanoi	0.9676	0.6904	0.5805	0.6503
	Danang	0.9377	0.5004	0.4314	0.5420
	Hochiminh	0.9695	0.6086	0.4772	0.6543

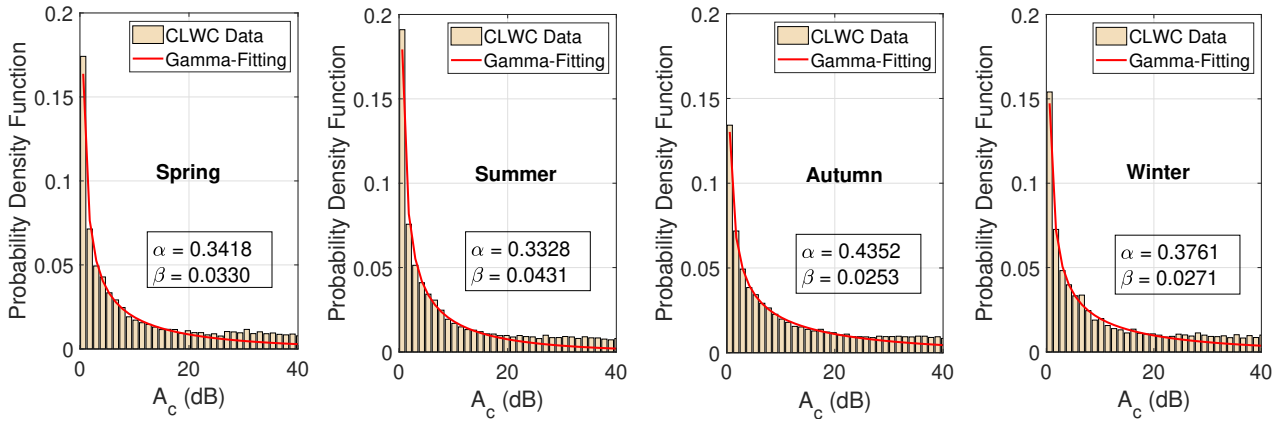


Figure 2. Statistical Log-normal distribution of cloud attenuation in 6 years (2015-2020) for Ha Noi region.

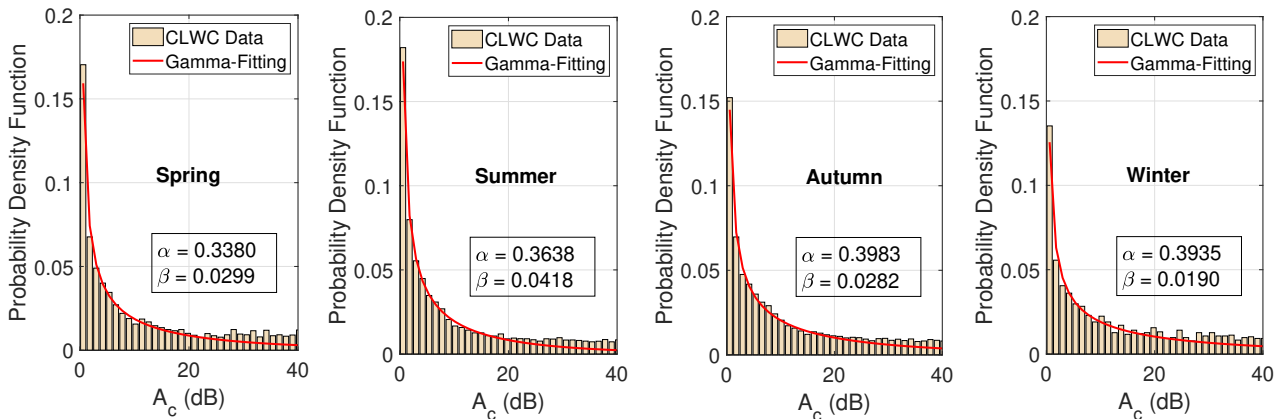


Figure 3. Statistical Log-normal distribution of cloud attenuation in 6 years (2015-2020) for Da Nang region.

4.1. Total Power Loss

Optical signals are susceptible to atmospheric problems, including atmospheric turbulence and cloud attenuation. The total power loss, denoted A_{total} caused by atmospheric turbulence A_{tur} and cloud attenuation

A_c , which can be defined as follows:

$$A_{\text{total}} = A_c + A_{\text{tur}} \quad (9)$$

A_c is given from (5). Let d be the communication distance from the satellite to the earth station, the loss caused by atmospheric disturbance A_{tur} can be

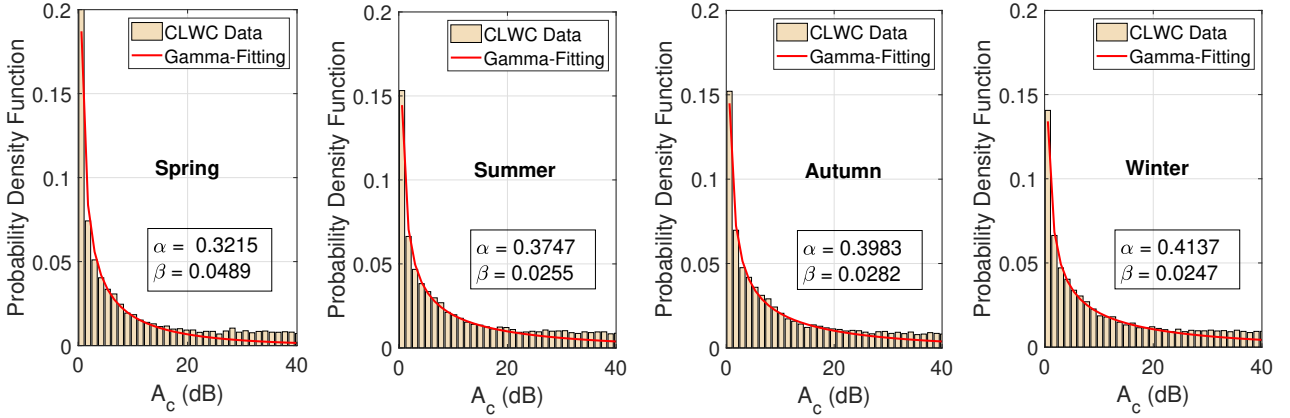


Figure 4. Statistical Log-normal distribution of cloud attenuation in 6 years (2015–2020) for Ho Chi Minh region.

expressed [25]

$$A_{\text{tur}} = 4.343 \left[\text{erfcinv}(2p_{\text{th}}) \sqrt{2 \ln(\sigma_p^2 + 1)} - \frac{1}{2} \ln(\sigma_p^2 + 1) \right], \quad (10)$$

where $\text{erfcinv}(\cdot)$ is the inverse error function, $\ln(\cdot)$ is the natural logarithm, and $p_{\text{th}} = 10^{-2}$ is determined through actual measurements as reported in [26, 27]. Besides, the power scintillation index, denoted as σ_p^2 , is determined as

$$\sigma_p^2 = \sigma_R^2 \left[1 + 0.33 \left(\frac{\pi D^2}{2\lambda d} \right)^{\frac{5}{6}} \right]^{-\frac{7}{5}}, \quad (11)$$

where D is the receiver aperture diameter.

4.2. System Availability

System availability P_{avai} is calculated based on the probability that the total loss A_{total} caused by atmospheric conditions and weather is less than a designed power budget A_{budget} for the system. Its closed form can be given as

$$\begin{aligned} P_{\text{avai}} &= \Pr(A_{\text{total}} \leq A_{\text{budget}}) \\ &= \Pr(A_c \leq A_{\text{budget}} - A_{\text{tur}}) \end{aligned} \quad (12)$$

where $A_{\text{budget}}(\text{dB})$ is the total power budget for the optical communication link between the satellite and the earth station previously designed to ensure the greatest possible system availability. Based on the cloud statistical model given in (8) and considering the threshold of availability is $A_{\text{th}}(\text{dB}) = A_{\text{budget}} - A_{\text{tur}}$, the

system availability is calculated as

$$\begin{aligned} P_{\text{avai}} &= \int_0^{A_{\text{th}}} f_{A_c}(A_c; \alpha, \beta) dA_c \\ &= \frac{1}{\beta^\alpha \Gamma(\alpha)} \int_0^{A_{\text{th}}} A_c^{\alpha-1} \exp\left(-\frac{A_c}{\beta}\right) dA_c, \end{aligned} \quad (13)$$

Let $t = A_c/\beta$ and applying incomplete gamma function definition as $\gamma(s, x) = \int_0^x t^{s-1} \exp(-t) dt$, (13) can be derived as

$$P_{\text{avai}} = \frac{\gamma(\alpha, A_{\text{th}})}{\Gamma(\alpha)}, \quad (14)$$

where $\gamma(\cdot, \cdot)$ is incomplete gamma function and $\Gamma(\cdot)$ is the gamma function.

4.3. Site Diversity Technique

The idea of the site diversity technique is simply based on the diversity of the same receiving signals from different earth stations. We assume that the stations in Vietnam are far away from each other enough to make the links be affected differently by atmospheric conditions. If the signal is heavily attenuated in some areas, other ground stations can compensate for it. Let N be the total number of earth stations available for satellite communication. The optical communication link availability A will be calculated when at least one earth station can communicate with the satellite, and it can be defined as

$$\begin{aligned} A &= 1 - \prod_{i=1}^N \Pr[A_{\text{loss}}(i) > A_{\text{budget}}] \\ &= 1 - \prod_{i=1}^N P_{\text{na}}(i), \end{aligned} \quad (15)$$

Table 2. α and β in different months.

Month	Para.	Ha Noi	Da Nang	Ho Chi Minh
Jan.	α	0.4243	0.3740	0.3122
	β	0.0237	0.0197	0.0542
Feb.	α	0.3225	0.3252	0.3203
	β	0.0447	0.0328	0.0551
Mar.	α	0.3322	0.3468	0.3365
	β	0.0358	0.0330	0.0400
Apr.	α	0.3329	0.3260	0.3649
	β	0.0570	0.0695	0.0276
May	α	0.3484	0.4213	0.6053
	β	0.0328	0.0321	0.0209
Jun.	α	0.3307	0.3764	0.3416
	β	0.0403	0.0435	0.0411
Jul.	α	0.3745	0.3908	0.4100
	β	0.0284	0.0366	0.0298
Aug.	α	0.4507	0.3834	0.4157
	β	0.0253	0.0303	0.0268
Sep.	α	0.5380	0.5005	0.3712
	β	0.0251	0.0238	0.0290
Oct.	α	0.4074	0.3239	0.4218
	β	0.0223	0.0179	0.0231
Nov.	α	0.3279	0.4535	0.4825
	β	0.0342	0.0188	0.0218
Dec.	α	0.4211	0.5248	0.3811
	β	0.0297	0.0273	0.0314

where P_{na} is defined as the probability that the i -th earth station cannot communicate with the satellite.

5. Numerical Results and Discussions

This section introduces step-by-step cloud attenuation distribution in three considered cities of Vietnam in 6 years (2015-2020), the system availability of those cities in different seasons, the comparison of the system availability between the tropical region (Vietnam) and temperate region (Japan), and the improvement of system availability when applying site diversity method.

Before looking at those results, some important parameters of the considered system are set as follows. The Stratus clouds are investigated, in which the mean of cloud droplet radius $r = 3.33\mu m$. As mentioned above, we divide the low clouds with an altitude of 1 to 3 km into 5 layers corresponding to the pressure levels, and $\Delta h = 0.5$ km. The optical wavelength, $\lambda = 1550$ nm, is used for this study. The histograms of the measured data are generated with $N = 50$ bins. The zenith angle is equal to 40° , the satellite's altitude is considered to be 514 km (equal to the altitude of Vietnam's Micro Dragon satellite), the receiver aperture diameter $D = 10$ cm, the height of the ground station is 10 m.

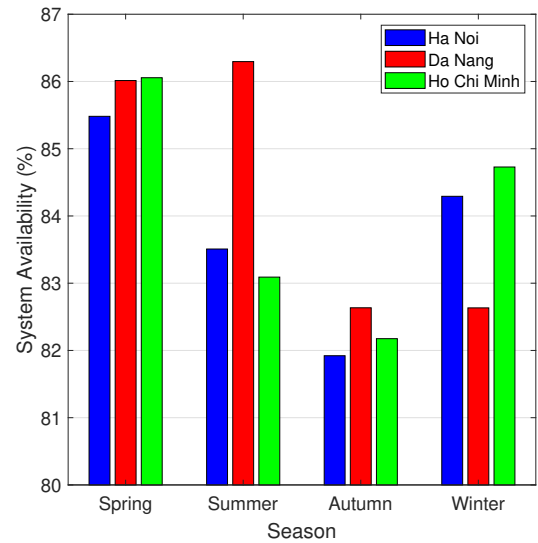


Figure 5. Availability of optical communication systems from satellites to earth stations under seasonal cloudiness.

Based on the fitting maximum likelihood estimation, we can get the values of α and β of the PDF of the cloud attenuation at each region in tropical region, which is given in Table 2. This table illustrates the monthly variations of α and β in tropical region with three main locations including Ha Noi, Da Nang, and Ho Chi Minh. As seen, these values exhibit remarkable monthly variations, which highlights the necessity of the monthly prediction model for the attenuation caused by clouds.

The first result shows the PDFs of the cloud attenuation in 6 years for Hanoi, Danang, and Hochiminh cities in Fig. 2, Fig. 3 and Fig. 4, respectively. In each city, the results are shown in four seasons (Spring, Summer, Autumn, and Winter) and achieved by two resources, the measured data, and the matching gamma distribution. In those pictures, the gamma model matches well with the measured data. In addition, based on the fitting maximum likelihood estimation, we can get the values of α and β for each season. Furthermore, these significant fluctuations of values in each season confirm the necessity of the estimation model for cloud attenuation.

The second result investigates the system availability of three major cities (Hanoi, Da Nang, and Ho Chi Minh City) with the effects of cloud attenuation but without atmospheric turbulence. Those cities are located in the north, middle, and south of Vietnam with different weather conditions and cloud coverage. The designed link budget is 30 dB to deal with cloud attenuation. As shown in Fig. 5, availabilities in all cities are lowest in autumn and highest in spring. Although the system

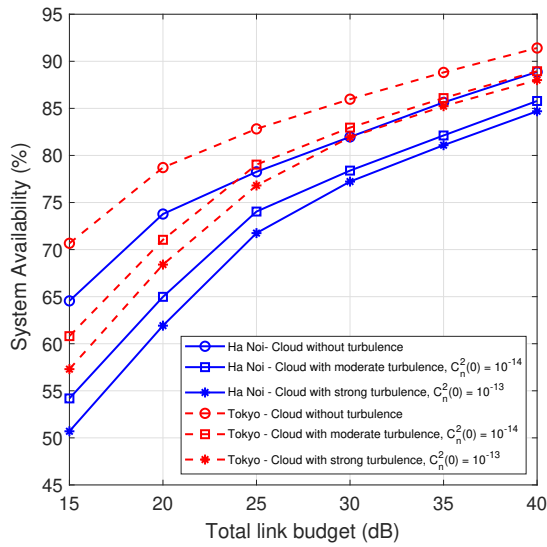


Figure 6. Availability of satellite-based FSO communication system between temperate (Tokyo - Japan) and tropical monsoon (Hanoi - Vietnam) climate zones during the rainy season in the period 2015 - 2020.

availability in Da Nang is highest in summer with a significantly better value, it becomes lowest in winter with a huge drop.

The third result shown in Figure 6 evaluates the system availability under the impact of atmospheric conditions (cloud attenuation and atmospheric turbulence) in two different climate zones of the temperate region (dashed line: Tokyo, Japan) and tropical region (solid line: Hanoi), Vietnam). There are three different atmospheric conditions, i.e., cloud effect only (dotted blue line), cloud effect with moderate turbulence (red dotted line), and clouds with strong turbulence (black line dotted with stars). In the figure, the system availability in Hanoi is always lower than in Tokyo in all three conditions. For example, with a designed power budget of 30 dB, the availability is 86%, 83%, and 82% in Tokyo for the three above conditions with no turbulence, moderate disturbance, and strong disturbances. However, they are only 81.96%, 78.39%, and 77.25% in Hanoi. The reason is that the weather in Hanoi is always hotter and more humid at the same time in Tokyo. So, clouds in Vietnam contain greater liquid water droplets than those in Tokyo. And the more water droplets clouds have, the more attenuation the lasercom suffers.

The last result, as shown in Figure 7, proves the effectiveness of applying site diversity to improve system performance in three cities in Vietnam. The designed power budget is 30 dB, and atmospheric conditions contain cloud attenuation and strong

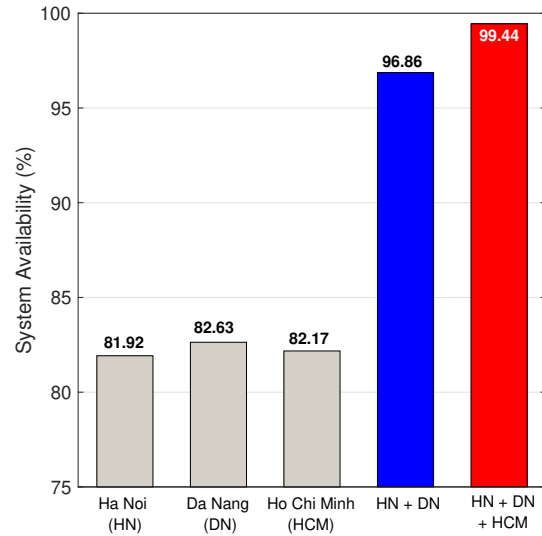


Figure 7. The system availability with the link budget of 30 dB is enhanced by the application of geographic station diversity.

atmospheric turbulence. The considered cloud data is in autumn (rainy season in Vietnam), the time of lowest availability, as shown in Figure 5. In Fig. 7, the system availability will be as low as 81.92%, 82.63%, and 82.17%, respectively, in the three individual cities. However, when applying the site diversity technique, stations in different cities are connected by a fiber-optic system. The more stations are connected, the system availability will increase accordingly. For example, if only two stations in Hanoi and Da Nang are connected, the availability will increase to 96.86%, especially when all stations in Hanoi, Da Nang, and Ho Chi Minh City are connected, the availability can be up to 99.44%, which is almost perfect. The result means that the proposed site diversity technique is truly effective in relaxing the effects of clouds and atmospheric turbulence.

6. Open Issues and Research Directions

We now identify the research direction and discuss the open issues for the mitigation techniques in the vision of future sixth-generation (6G) wireless networks. For satellite laser communications, the presence of opaque clouds may occasionally disrupt the signal or completely block the optical signal from ground to satellite or satellite-to-ground rendering the LOS communication useless, as we discussed above. These intermittent blockages can last from a few seconds to several hours, depending on the geographical location and season. They can lead to wandering off the downlink signal from the desired position if the spaceborne system relies on an uplink beacon signal for

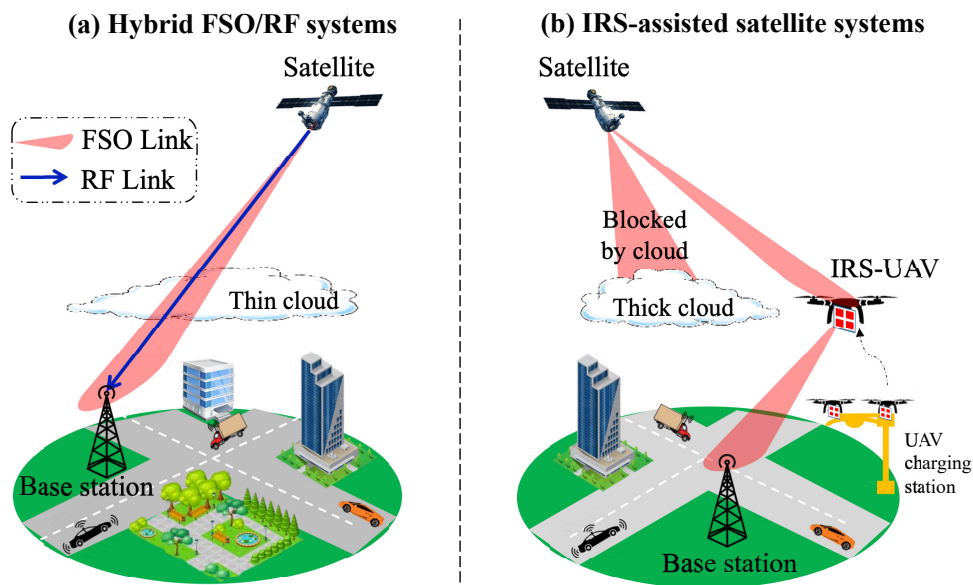


Figure 8. The mitigation techniques for the impact of cloud coverage: (a) Hybrid FSO/RF system and (b) IRS-assisted satellite system.

tracking and pointing. Cumulus clouds may appear alone or in clusters in the altitude range from 50 to 2000 meters above the ground and hinders satellite laser communication. Clouds cause significant attenuation as high as tens of dB and therefore require necessary actions to counteract the power loss due to cloud coverage. While site diversity is usually applied in large-scale networks, e.g., countries, the mitigation techniques for small-scale networks, e.g., rural areas, disaster areas, remote areas, etc., need to investigate. Figure 8 describes two proposed techniques in different cloud conditions. In the situation of a thick cloud, as shown in Fig. 8, an emerging technique, namely intelligent reflecting surface-unmanned aerial vehicle (IRS-UAV), is deployed to maintain the satellite laser communication. In the case of thin clouds, the hybrid FSO/radio frequency (RF) system can be used since the RF technology is not affected by clouds due to the characteristic of the RF wavelength. There are several practical transmission schemes for hybrid FSO/RF systems, such as single switching-based hybrid FSO/RF transmission schemes, hybrid FSO/RF systems with adaptive combining, and adaptive rate for hybrid FSO/RF systems.

Our study provides a method for analyzing the impact of atmospheric and weather conditions, i.e., cloud coverage in satellite FSO laser communications. This analysis is not limited to satellites but also to other platforms such as high-altitude platforms (HAP), e.g., balloons, commercial aircraft, aircraft, or other low-altitude platforms (LAP), e.g., drones, helicopters. Besides, ground stations are not only fixed but also

moving ones, such as ships, self-driving cars, and high-speed trains. For future outlook, we plan to build a framework for the FSO communication channel model with the combination of the effect of weather conditions in addition to other impact factors from transmitter and receiver such as the satellite vibration, the UAV hovering, the speed of a self-driving car or a high-speed train.

7. Concluding Remarks

The ultimate goal of our research is to evaluate the availability of satellite lasercom links under two main effects, including clouds and atmospheric turbulence in tropical regions. The statistical model of cloud attenuation was derived based on the cloud database collected by the ECMWF. The result reveals that the Gamma distribution matches well with the observed CLWC data. Based on the derived cloud attenuation, the system availability is analyzed in detail for several areas in tropical regions, including Hanoi, Danang, and Hochiminh. In all investigated cities, the system availability depending on the link budget is below 90% with the link budget smaller than 40 dB. Site diversity seems to be an effective solution to the cloud problem. It helps to increase the system availability up to 99.44% when three sites are used.

References

- [1] LE, H.D. and PHAM, A.T. (2022) Link-layer retransmission-based error-control protocols in FSO communications: A survey. *IEEE*

- Commun. Surveys & Tutorials* 24(3): 1602–1633. doi:10.1109/COMST.2022.3175509.
- [2] TOYOSHIMA, M. (2021) Recent trends in space laser communications for small satellites and constellations. *J. Lightw. Technol.* 39(3): 693–699.
 - [3] NGUYEN, T.V., LE, H.D., DANG, N.T. and PHAM, A.T. (2021) On the design of rate adaptation for relay-assisted satellite hybrid FSO/RF systems. *IEEE Photonics J.* : 1–1 doi:10.1109/JPHOT.2021.3130720.
 - [4] GHASSEMLOOY, Z., ARNON, S., UYSAL, M., XU, Z. and CHENG, J. (2015) Emerging optical wireless communications—advances and challenges. *IEEE J. Sel. Areas Commun.* 33(9): 1738–1749.
 - [5] AKYILDIZ, I.F., KAK, A. and NIE, S. (2020) 6G and beyond: The future of wireless communications systems. *IEEE Access* 8: 133995–134030.
 - [6] (2020), Natural disasters 2019: Now is the time to not give up, Centre for Research on the Epidemiology of Disaster (CRED), Brussels.
 - [7] LE, H.D., NGUYEN, T.V. and PHAM, A.T. (Feb. 2021) Cloud attenuation statistical model for satellite-based FSO communications. *IEEE Antennas Wireless Propag. Lett.* 20(5): 643–647.
 - [8] NGUYEN, T.V., LE, H.D., PHAM, T.V. and PHAM, A.T. (Feb. 2021) Link availability of satellite-based FSO communications in the presence of clouds and turbulence. *IEICE Commun. Exp.* 10.
 - [9] SUZUKI, K., KOLEV, D.R., CARRASCO-CASADO, A. and TOYOSHIMA, M. (2018) Environmental-data collection system for satellite-to-ground optical communications. *Trans. JSASS Aerosp. Tech. Japan* 16(1): 35–39.
 - [10] LYRAS, N.K., KOUROGIORGAS, C.I. and PANAGOPOULOS, A.D. (Sep. 2017) Cloud attenuation statistics prediction from Ka-band to optical frequencies: Integrated liquid water content field synthesizer. *IEEE Trans. Antennas Propag.* 65(1): 319–328.
 - [11] LYRAS, N.K., EFREM, C.N., KOUROGIORGAS, C.I., PANAGOPOULOS, A.D. and ARAPOGLOU, P.D. (Oct. 2020) Optimizing the ground network of optical MEO satellite communication systems. *Syst. J.* 14(3): 3968–3976.
 - [12] SUZUKI, K., KUBOOKA, T., FUSE, T., YAMAMOTO, S., KUNIMORI, H. and TOYOSHIMA, M. (2014) Environmental data gathering system for satellite-to-ground station optical communications. In *Proc. IEEE Int. Conf. Space Opt. Syst. Appl. (ICSOS)*: 1–6.
 - [13] KOLEV, D.R., CARRASCO-CASADO, A., SUZUKI, K. and TOYOSHIMA, M. (2017) Environmental-data collection system testbed for site-diversity implementation in satellite-to-ground laser communications. In *Proc. IEEE Int. Conf. Space Opt. Syst. Appl. (ICSOS)*: 286–289.
 - [14] LYRAS, N.K., KOUROGIORGAS, C.I. and PANAGOPOULOS, A.D. (Mar. 2017) Cloud free line of sight prediction modeling for optical satellite communication networks. *IEEE Commun. Lett.* 21(7): 1537–1540.
 - [15] LYRAS, N.K., EFREM, C.N., KOUROGIORGAS, C.I. and PANAGOPOULOS, A.D. (Mar. 2018) Optimum monthly based selection of ground stations for optical satellite networks. *IEEE Commun. Lett.* 22(6): 1192–1195.
 - [16] NGUYEN, T.V., PHAM, T.V., DANG, N.T. and PHAM, A.T. (2020) Performance of generalized QAM/FSO systems with pointing misalignment and phase error over atmospheric turbulence channels. *IEEE Access* 8: 203631–203644.
 - [17] KAUSHAL, H. and KADDOUM, G. (Jan. 2017) Optical communication in space: Challenges and mitigation techniques. *IEEE Commun. Surveys Tuts.* 19(1): 57–96.
 - [18] NGUYEN, T.V., PHAM, T.V., DANG, N.T. and PHAM, A.T. (2020) UAV-based FSO systems using SC-QAM signaling over fading channels with misalignment. In *Proc. IEEE 92nd Veh. Technol. Conf. (VTC2020-Fall)*: 1–5.
 - [19] ECMWF, ERA-interim database. Accessed: 19-05-2022. [Online]. Available: <https://apps.ecmwf.int/datasets/data/interim-full-daily>.
 - [20] ALZENAD, M., SHAKIR, M.Z., YANIKOMEROGLU, H. and ALOUINI, M. (Jan. 2018) FSO-based vertical backhaul/fronthaul framework for 5G+ wireless networks. *IEEE Commun. Mag.* 56(1): 218–224.
 - [21] YIN, J.F., WANG, D.H., ZHAI, G.Q. and XU, H.B. (Mar. 2014) An investigation into the relationship between liquid water content and cloud number concentration in the stratiform clouds over north china. *Elsevier Atmospheric Research* 139(1): 137–143.
 - [22] ERDOGAN, E., ALTUNBAS, I., KURT, G.K., BELLEMARE, M., LAMONTAGNE, G. and YANIKOMEROGLU, H. (2021) Site diversity in downlink optical satellite networks through ground station selection. *IEEE Access* 9: 31179–31190.
 - [23] KIM, I.I., McARTHUR, B. and KOREVAAR, E.J. (2001) Comparison of laser beam propagation at 785 nm and 1550 nm in fog and haze for optical wireless communications. In *Proc. SPIE Opt. Wireless Commun. III*, 4214: 26–37.
 - [24] ANDREWS, L.C. and PHILLIPS, R.L. (2005) *Laser Beam Propagation through Random Media* (Bellingham, WA: SPIE Press), 2nd ed.
 - [25] GIGGENBACH, D. and MOLL, F. (2017) Scintillation loss in optical low earth orbit data downlinks with avalanche photodiode receivers. In *Proc. IEEE Int. Conf. Space Opt. Syst. Appl. (ICSOS)*: 115–122.
 - [26] GIGGENBACH, D. and HENNIGER, H. (2008) Fading-loss assessment in atmospheric free-space optical communication links with on-off keying. *Opt. Eng.* 47(4): 1 – 6. doi:10.1117/1.2903095, URL <https://doi.org/10.1117/1.2903095>.
 - [27] GIGGENBACH, D. and MOLL, F. (2017) Scintillation loss in optical low earth orbit data downlinks with avalanche photodiode receivers. In *Proc. IEEE Int. Conf. Space Opt. Syst. Appl. (ICSOS)*: 115–122. doi:10.1109/ICSOS.2017.8357220.